Gravity and Magnetic Signatures of Different Types of Spreading at the Mid-Atlantic Ridge

Gabriella Alodia*[1], Chris Green[1,2], Andrew McCaig[1], Douglas Paton[1], and Simon Campbell[2]
[1]School of Earth and Environment, University of Leeds, UK; [2]Getech, plc., Leeds, UK

AGU FALL MEETING New Orleans | 11-15 December 2017

lembaga pengelola dana pendidikan lpdp

getech

Basin Structure Group Petroleum Leeds

UNIVERSITY OF LEEDS

1. Introduction

In recent years it has been recognised that parts of slow spreading ridges such as the Mid-Atlantic Ridge (MAR) are characterised by typical magmatic spreading, while other parts are characterised by the formation of detachment faults and Oceanic Core Complexes (OCC). These different spreading modes can be clearly identified in the near-ridge environment in the bathymetry, with magmatic mode crust characterised by linear fault-bounded ridges, and detachment mode crust by more chaotic bathymetric signatures. The aim of this project is to characterise the magnetic and gravity signatures of lithosphere created by different modes of spreading, with the aim of using these signatures to identify if the structures still remain in ocean-continent transitions, where they have been covered by sediments coming from the continental crust.

We first characterise different modes of spreading using available high-resolution bathymetry data of the MAR up to 20 My of age. The identified characteristics are then related to the corresponding ship-borne gravity and magnetic data in the same area. From the gravity anomalies, thinner crust is observed where the OCCs are in place. This allows the mantle to be exhumed to the sea-floor. As for the magnetic anomalies, it is found that in places where OCCs are present, the anomalies are not as symmetrical as those found in magmatic mode regions. We present a range of parameters extracted from the data that characterise different spreading modes, and use these to test whether transitions between detachment and magmatic mode crust identified in the bathymetry can be readily identified in gravity and magnetic data.

2. Mid-Atlantic Ridge Spreading Modes

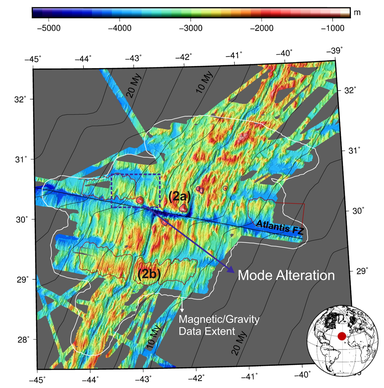

Two different modes of spreading in the MAR, denoted as detachment fault and magmatic modes, are identified in our study area: the Atlantis Fracture Zone (FZ). Both modes are distinguished by the morphology of the seabed. For example, sporadic massifs are found within the young lithosphere in the vicinity of Atlantis FZ to the north, while abyssal hills are found in both the southern area and in the older section of the lithosphere in the vicinity of the FZ. This indicates that these modes could alternate from one to another.

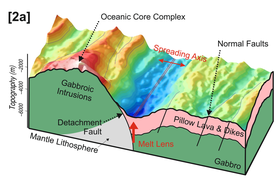

[2a] Detachment Fault Mode. Identified where sporadic massifs, known as OCCs, are in place. OCCs represent exhumed rocks from the lower-crust to the upper-mantle layers like gabbros and peridotites, activated by so-called detachments faults. The fault started off as a normal fault that grew weaker and got rolled back towards the spreading direction, resulting in asymmetrical features.

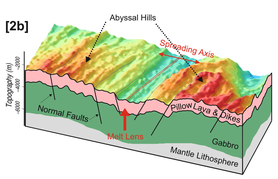

[2b] Magmatic Mode. It is identified where relatively symmetrical abyssal hills are in place on boths sides of the ridge. These indicate that both sides developed in relatively similar time, strengthened by the presence of relatively symmetrical normal faults on both sides and neatly stacked layers from the pillow lavas and dikes, down to the gabbro and mantle lithosphere layers.

*Contact: eega@leeds.ac.uk

Acknowledgement

This poster is part of a PhD project carried out under the School of Earth and Environment, University of Leeds, starting from October 2016 and expected to be completed over a period of 3-4 years. The whole training is funded by the Indonesian Endowment Fund for Education (LPDP) and supported by Getech, plc. as a project partner which provides several data set and licensed software. Other data are obtained both from open source data repositories (LDEO's IEDA, NOAA's NCEI Trackline, and GMRT MapTool) and direct contact with Johnson R. Cann, Deborah K. Smith, Donna Blackman, and Javier Escartin.

3. Lithospheric Cooling Model and Thermal Gravity Anomalies

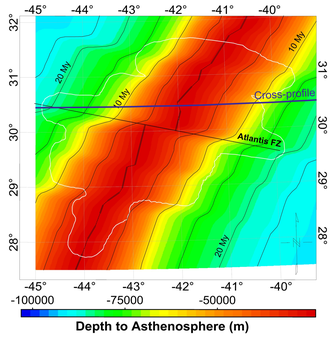

Lithospheric cooling model using 'plate model' equation, overlayed by Age of Lithosphere (black, My) and data extent (white).

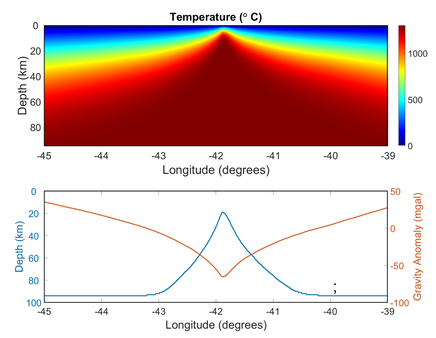

Cross-profiles at 30.5°N latitude. Top: Temperature distribution (°C). Bottom: Depth to lithosphere (km) and thermal gravity anomaly (mgal).

At a spreading ridge, we need to take into account the gravity anomalies that result from the cooling of the oceanic lithosphere. A lithospheric model is constructed using the 'plate model' equation from Turcotte & Schubert (2002). Here we put y, the maximum plate thickness, as 95 km which is the maximum plate thickness of the GDH1 Plate Model (Richardson, et al., 1995). The upper and lower temperature boundaries are $T_0 = 0°C$ and $T_m = 1300°C$ respectively. We take $\kappa = 10^{-6}\ Wm^{-1}K^{-1}$ as the coefficient of thermal conductivity, with varying age t from Müller et al. (2008) and depth b of 1 km spacing for every discrete layer.

$$T = (T_i - T_0)erf\left(\frac{y}{2\sqrt{\kappa t}}\right) + \frac{(T_{i+1} - T_i)}{2} \times \left\{erf\left(\frac{y-b}{2\sqrt{\kappa t}}\right) + erf\left(\frac{y+b}{2\sqrt{\kappa t}}\right)\right\} + T_0$$

Using a thermal expansion coefficent $\alpha = 3 \times 10^{-5}$ K (Kuo & Forsyth, 1988), thermal gravity anomalies could then be computed by first expressing the density contrast (Chappell & Kusznir, 2008).

$$\Delta T = T_i - T_m \times \frac{z_i}{y} \qquad \Delta\rho = -\alpha\rho\Delta T$$

For the lithosphere thickness/depth, as we set the lower, i.e. the mantle boundary to 1300°C, the depth of the lithosphere is then expressed by the 1300°C contour in the resulting model, which is flattened when it reached the maximum plate thickness.

4. Gravity: Residual Crustal Thickness

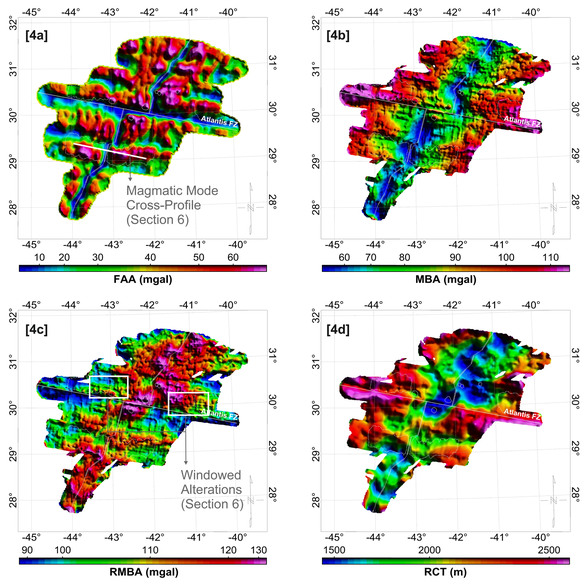

Vatiation of crustal thicknes, i.e. Moho depth, can be calculated by examining variations of gravity in different reference levels. In this model, we assume that the sediment layer is very thin, hence its gravity attraction is negligible.

[4a] Free Air Anomaly (g_{FAA}): gravity anomaly from the observation point, i.e. water level.

[4b] Mantle Bouguer Anomaly (g_{MBA}): gravity anomalies obtained by subtracting from the g_{FAA} the attraction of the topography (removing effects from *upward continued* bathymetry) and of an assumed homogenous 6 km thick crust (as a first approach of Moho depth). The anomalies here no longer mimics the sea floor, but negative anomalies depicting the cooling of the oceanic lithosphere are still quite dominant.

[4c] Residual Mantle Bouguer Anomaly (g_{RMBA}): gravity anomalies obtained by subtracting from the g_{MBA} the attraction from the cooling of the lithosphere (g_T), obtained from Section 3. The anomalies are no longer depicting the ridge, hence the only attraction that is left would serve as an approach of to observe the crustal thickness variation.

[4d] Residual Crustal Thickness (RCT): the vertical difference between the assumed homogenous 6 km thick crust to the 'real' depth of the Moho. This is obtained by adding the inverted g_{RMBA} signals to the assumed crustal depth of 6 km. The depth of the Moho itself will act as on of the most important horizon in the model. Based on this result, we can see that the detachment fault zone tend to have thinner crust than the magmatic zone. Alteration from one mode to another can still be seen, especially north of Atlantis FZ.

5. Magnetic: Anomalies and Dip Anisotropy

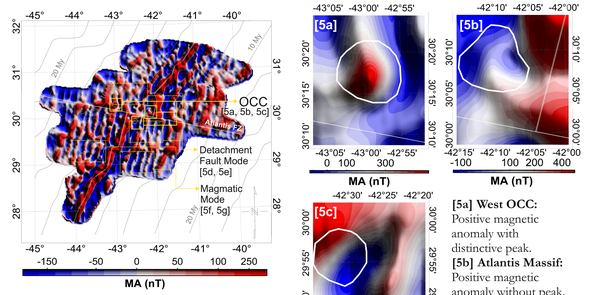

Three OCCs are windowed in [5a-5c] to constrain the local signatures, while [5d-5g] are windowed to see the magnetic dips in both spreading modes.

[5a] West OCC: Positive magnetic anomaly with distinctive peak.
[5b] Atlantis Massif: Positive magnetic anomaly without peak.
[5c] South OCC: Adjacent to negative magnetic anomaly with distinct 'valley.'

Based on our observation in **[5a-5c]**, we found that magnetic signatures do not always behave similarly where OCCs are in place. We hypothize that positive Magnetic Anomaly (MA) is found around active OCC(s) while negative MA is found around inactive one(s).

We also characterize the different types of spreading by examining the dip anisotropy, i.e. the directional components. In **detachment fault mode [5d-5e]**, the magnetic anomaly (stripes) is scattered, blobby, with reversals that are not clearly seen. The polar histograms also depict the undulation in the directions other than the original WNW-ESE dip. While in **magmatic mode [5f-5g]**, the stripes have more consistent texture with clearly seen reversals. Both polar histograms depict mostly the WNW-ESE dip with minor undulations in other directions.

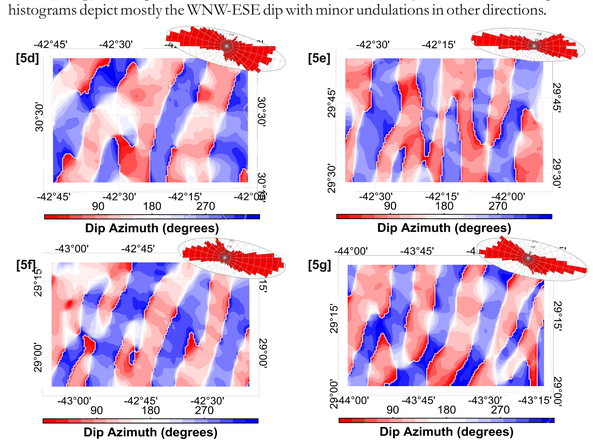

6. Mode Alteration and Model Building

In our study area, we found out that there is a possibility of alteration from one spreading mode to another. This is observable both in the bathymetry and gravity (in this case, RMBA). The area of alteration tend to be symmetrical, i.e. situated within similar age on both sides of the ridge. This means that, detachment faulting actually also occurred 'symmetrically' even though the OCCs are only in place on one side of the ridge. Also, we could say that if we found magmatic terrain on one side of the ridge, it is probably also in place in another side within the similar age.

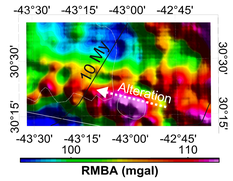

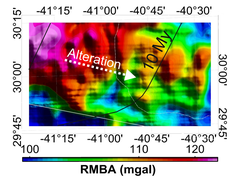

Afterwards, we built a cross-profile model (2D) of the magmatic terrain with layers/rocks as depicted in the table below. Moho depth is calculated by adding the assumed "Moho depth" of 6 km with the RCT from Section 4, which results coincides with the depth of the Ultramafics layer. The depth to asthenosphere is defined by the lithosphere thickness from Section 3. The physical properties of each layer is also depicted in the table (thickness h, density ρ, susceptibility χ) used in the model are simplified from Hunt, et al. (1995).

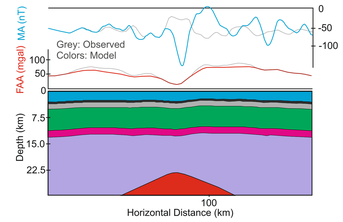

Physical properties of each layer.

	Layers/Rocks	h (km)	ρ (g/cm^3)	χ (SI)
A	Sea Water	0.0	1.03	0.00
B	Basaltic Pillow Lava	0.5	2.99	0.09
C	Diabase Dikes	1.5	2.91	0.08
D	Gabbro	2-5	3.03	0.04
E	Ultramafics	2-5	3.15	0.06
F	Lower Lithosphere	Varies	3.30	0.00
G	Asthenosphere	Varies	3.20	0.00

It appears that using the information given in the table we could obtain an FAA response which coincides well with the observed one. As for MA, it is not quite straight forward as a lot of lateral variations are already observed in the MA response. This depiction might be due to the strength of the remanence magnetism. Hence the subsequent magnetic response model need to take into account both remanence and induced magnetism.

7. Conclusions and Further Works

Conclusions

- Thinner crust is identifiable in detachment mode of spreading. In this area, it is ~1 km thinner than in magmatic mode. This finding is consistent with previous published works on the differentiation between one spreading mode to another.
- The dips of the magnetic anomalies in detachment mode of spreading tend to be more anisotropic than in magmatic mode. Blobby textures with unclear magnetic reversals are expected, in contrast with consistent and symmetrical textures observed in magmatic mode.
- Gravity response of the model coincides well with slightly higher amplitude on peaks. These are depicted as the model is still being built 2-dimensionally, thus the lateral effect are still there. This amplitude difference is not to be expected in the 3-dimensional models.
- Lateral changes, both/either in magnetic remanence and/or susceptibility need to be included in the physical model in order to have the expected magnetic response.

Further Works

- Test if the findings are still consistent in other area(s) which has similar data quality, followed by testing in area(s) which only consist of global/satellite-derived data.
- Test models in area(s) in which seismic survey(s) has/have been carried out.
- Construct 3-dimensional models.

References

Hunt, C. P., Moskowitz, B. M., & Banerjee, S. K. (1995). Magnetic Properties of Rocks and Minerals. *Rock Physics and Phase Relations: A Handbook of Physical Constants, AGU Reference Shelf* 3, 189-204.

Kuo, B. Y., & Forsyth, D. W. (1988). Gravity anomalies of the ridge-transform system in the South Atlantic between 31 and 34.5 S: Upwelling centers and variations in crustal thickness. *Marine Geophysical Research*, 10(3), 205-232.

Müller, R. D., Sdrolias, M., Gaina, C., & Roest, W. R. (2008). Age, spreading rates, and spreading asymmetry of the world's ocean crust. *Geochemistry, Geophysics, Geosystems*, 9(4).

Richardson, W. P., Stein, S., Stein, C. A., & Zuber, M. T. (1995). Geoid data and thermal structure of the oceanic lithosphere. *Geophysical research letters*, 22(14), 1913-1916.

Smith, D. K., Escartín, J., Schouten, H., & Cann, J. R. (2008). Fault rotation and core complex formation: Significant processes in seafloor formation at slow-spreading mid-ocean ridges (Mid-Atlantic Ridge, 13–15 N). *Geochemistry, Geophysics, Geosystems*, 9(3).

Turcotte, D. L., & Schubert, G. (2002). *Geodynamics*, 456 pp.